



Effect of Phase Angle Unbalance on Working Characteristics of LSPMSM During Transient Process

L. A. Tuan^a, D. Y. Nhu^b, N. T. Khanh^{*b}

^a School of Electrical and Electronic Engineering, Hanoi University of Industry, Hanoi, Vietnam

^b Faculty of Electro-Mechanics, Hanoi University of Mining and Geology, Hanoi, Vietnam

PAPER INFO

Paper history:

Received 24 January 2025

Received in revised form 21 February 2025

Accepted 24 March 2025

Keywords:

Line-start Permanent Magnet Synchronous Motors

Electrical Motor

Permanent Magnet

Power Quality

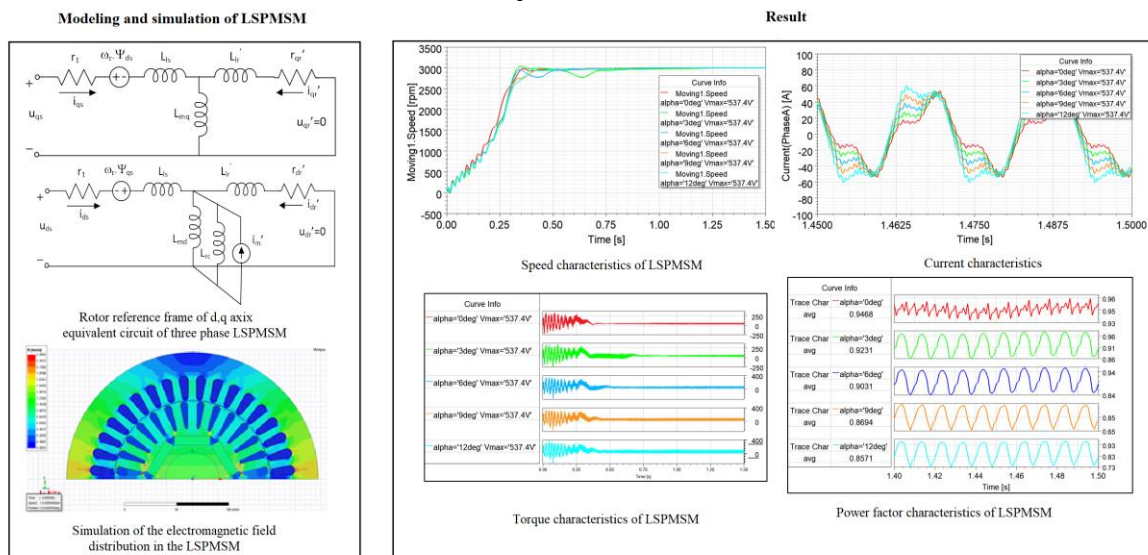
Phase Angle Unbalance

ABSTRACT

Nowadays, line-start permanent magnet synchronous motors (LSPMSM) are being researched as a partial replacement for induction motors for energy-saving purposes. The LSPMSM is typically designed to operate with three-phase voltage balance (VB). Currently, with single-phase loads, the phenomenon of phase angle unbalance (PAU) frequently occurs in the distribution network, which deteriorates the working parameters of the motor and may lead to damage during operation. Therefore, the content of this paper focuses on studying the impact of PAU in the distribution network on the working characteristics of LSPMSM 15 kW- 3,000 rpm. The analysis results show that when PAU occurs, the LSPMSM has more difficulty starting and may not start. The LSPMSM speed fluctuates strongly, does not work at synchronous speed and mainly works in transient process. During the transient process leads to a higher oscillation torque coefficient k , which explains that the motor will operate with more vibration and acoustics noise. Furthermore, the effect of PAU increases losses, reducing the efficiency and power factor of the motor. The paper evaluates this effect through simulation models and experimental testing in the laboratory for the LSPMSM. The results demonstrate that the theoretical basis synthesized in the paper is suitable for the study.

doi: 10.5829/ije.2026.39.02b.13

Graphical Abstract



*Corresponding Author Email: nguyenthackhanh@humg.edu.vn (N. T. Khanh)

Please cite this article as: Tuan LA, Nhu DY, Khanh NT. Effect of Phase Angle Unbalance on Working Characteristics of LSPMSM During Transient Process. International Journal of Engineering, Transactions B: Applications. 2026;39(02):454-64.

1. INTRODUCTION

Currently, energy saving is becoming a global issue as fossil energy sources are gradually depleting and causing environmental pollution (1). Electric motors, particularly induction motors (IM), account for up to 46% of electrical energy consumption (2, 3). With the development of rare earth magnets, the replacement of low-efficiency motors with high-efficiency ones is becoming a global trend. Line-start permanent magnet synchronous motors (LSPMSM) are increasingly replacing lower-efficiency IMs (4).

The LSPMSM is a hybrid design that combines the squirrel-cage induction motors (SCIM) with the permanent magnets synchronous motors (PMSM) (5). Due to the squirrel cage, the motor can be directly started from the power supply and operates at synchronous speed in steady state, thus eliminating resistive losses in the rotor and resulting in high efficiency (6). Like other motors, the LSPMSM is significantly affected by the power quality provided to it during operation. The impact of voltage unbalance (VU) in both amplitude and phase angle of the voltage on the efficiency and current characteristics of the LSPMSM under no-load, light-load, full-load, and overload conditions is demonstrated by Ferreira et al. (7). The research results show that efficiency, power factor, and current are all affected under conditions of VU and varying loads, particularly when voltage reduction significantly decreases the motor's load. Additionally, in all load modes, the harmonic levels of the current are high.

On the distribution network, the power supply in the industrial sector often simultaneously feeds both three-phase and single-phase electrical loads. Supplying single-phase loads or unbalance three-phase loads can lead to PAU in the distribution network (8). This power supply to the LSPMSM can degrade the operational quality of the motor and sometimes cause unwanted damage during operation (7). Researching the impact of power quality on the performance of electric motors in general, and LSPMSM in particular, is currently a focus, with the aim of developing solutions to enhance operational efficiency and minimize undesirable incidents.

Studies on the impact of power quality on LSPMSM can be categorized as follows: Tshoombe et al. (9), Gnaciński (10), Chingale and Ugale (11) investigated the effects of voltage quality, including voltage harmonics and voltage imbalance, on performance. These papers analyzed and indicated the extent of the impact of harmonics on the efficiency and vibration during the operation of LSPMSM. Ugale et al. (12), Qiu et al. (13) and Gnaciński et al. (14) explored the effects of voltage flicker and high-frequency components on the operating conditions and efficiency of LSPMSM. Idziak et al. (15), examined the impact of stator current harmonic spectrum

when the motor operates under VU with various load types. They found that the harmonic components of the current under conditions of amplitude voltage asymmetry ranging from 0 to 5% in the case of load variations.

Sethupathi et al. (16), Sethupathi and Senthilnathan (17) studied the finite element analysis (FEA) method; they used to analyze the impact of harmonics on stator losses and rotor losses in LSPMSM. Sethupathi and Senthilnathan (17) confirmed that under abnormal conditions of power quality, various mechanical anomalies such as vibrations, noise, and excessive temperature will occur, reducing the efficiency and lifespan of the motor. The efficiency of the LSPMSM decreases by up to 3.2%, and the input power increases by 102W in the case of a source voltage reduction of 19V and a VU of 5% for a 2.2kW, 4-pole motor. Paramonov et al. (18) demonstrated the effects of voltage drop as well as cable length on the starting process of centrifugal pumps.

The operating characteristics of the LSPMSM under conditions of stator winding asymmetry in no-load and full-load cases were studied by Maraaba et al. (19). The research results in the paper indicate that the parameters of the LSPMSM are affected not only by the phenomenon of stator winding asymmetry but also by the motor load, which impacts the operating parameters of the motor. A general model for LSPMSM under structural asymmetry presented in literature (20-22). The research results indicate that under conditions of stator winding asymmetry, the phenomenon of torque oscillation increases and the starting quality of the motor decreases. Ugale et al. (23), Huang and Wang (24) analyzed the impact of rotor materials and structure on the operational efficiency of the motor and proposed several solutions to enhance the performance of LSPMSM.

The effects of stator winding types and short circuits at certain stator windings were examined by Qiu et al. (25) and Fonseca et al. (26), which led to the occurrence of third-order harmonics during the operation of the motor. Additionally, the research evaluated the levels of losses and starting capabilities when the LSPMSM is connected in either star or delta configurations. The vibration phenomenon of the LSPMSM powered by an electrical source containing harmonics which was studied by Fonseca et al. (26). The paper discusses the analysis, and the research results indicate that the influence of voltage subharmonics causes significant vibrations in the motor, especially under full-load conditions.

From the above studies, it can be observed that researching the impact of factors related to power quality on the working conditions of LSPMSM is currently a significant issue. However, there has yet to be any study that provides a detailed analysis of the effects of PAU on the working conditions of LSPMSM. Although PAU is a common phenomenon affecting power quality in distribution networks, the content of this paper will

analyze the impact of PAU on the operation of LSPMSM in the case of operating with rated load, aiming to propose solutions to enhance the efficiency of the motors. To clarify the research issue, the paper will analyze the impact of phase unbalance on the LSPMSM. It will then utilize the finite element method based on Ansys Maxwell software to simulate and evaluate the 15kW-3000rpm LSPMSM, followed by experimental assessment in the laboratory.

2. THE EFFECT OF PAU ON LSPMSM

2.1. LSPMSM Model The mathematical model of the LSPMSM is expressed in the d-q coordinate system, with the applicable input parameters presented as follows (27, 28):

$$\begin{cases} u_{ds} = r_1 i_{ds} + \frac{d\Psi_{ds}}{dt} - \omega_r \cdot \Psi_{qs} \\ u_{qs} = r_1 i_{qs} + \frac{d\Psi_{qs}}{dt} + \omega_r \cdot \Psi_{ds} \end{cases} \quad (1)$$

$$\begin{cases} u'_{dr} = r'_{dr} i'_{dr} + \frac{d\Psi'_{dr}}{dt} = 0 \\ u'_{qr} = r'_{qr} i'_{qr} + \frac{d\Psi'_{qr}}{dt} = 0 \end{cases} \quad (2)$$

$$\begin{cases} \Psi_{ds} = (L_{ls} + L_{md})i_{ds} + L_{md}i'_{dr} + \Psi'_m \\ \Psi_{qs} = (L_{ls} + L_{mq})i_{qs} + L_{mq}i'_{qr} \end{cases} \quad (3)$$

$$\begin{cases} \Psi'_{dr} = L'_{lr}i'_{dr} + L_{md}(i_{ds} + i'_{dr}) + \Psi'_m \\ \Psi'_{qr} = L'_{lr}i'_{qr} + L_{mq}(i_{qs} + i'_{qr}) \end{cases} \quad (4)$$

where: ω_r - rotor angular velocity; Ψ'_m - stator flux generated by the permanent magnets ; L_{ls} - Leakage inductance of the stator winding; L_{md} and L_{mq} are magnetizing inductances of d, q axes; i_{ds} , i_{qs} - stator current of d, q axes; i'_{dr} , i'_{qr} - rotor equivalent current of d, q axes.

From Equations 1 to 4, an equivalent circuit diagram of the LSPMSM can be constructed, satisfying the voltage and flux equations in the mathematical model shown in Figures 1 and 2 (27).

Where, $\Psi'_m = L_{rc} \cdot i'_m$, L_{rc} is the fictitious reactance of the permanent magnet, and i'_m is the equivalent magnetizing current converted to the stator side of the

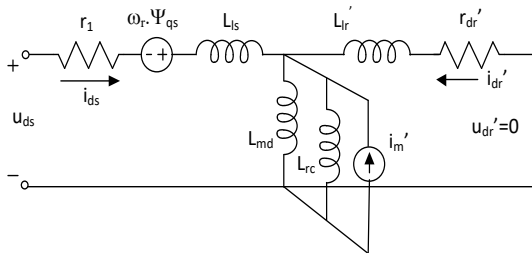


Figure 1. d - axis equivalent circuit of LSPMSM

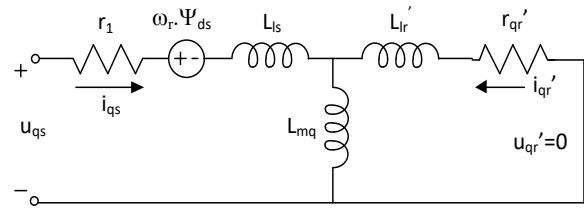


Figure 2. q - axis equivalent circuit of LSPMSM

permanent magnet. The electromagnetic torque of the LSPMSM is defined.

$$M_{el} = \frac{3}{2} \cdot p \cdot \left[\begin{matrix} (L_{md} \cdot i'_{dr} \cdot i_{qs} - L_{mq} \cdot i'_{qr} \cdot i_{ds}) \\ T_{ind} \\ + \Psi'_m \cdot i_{qs} + (L_{md} - L_{mq}) \cdot i_{ds} \cdot i_{qs} \\ T_{Exc} \quad T_{rel} \end{matrix} \right] \quad (5)$$

Thus, the electromagnetic torque of the LSPMSM consists of three components: T_{ind} - the induction torque component; T_{exc} - the excitation torque component; T_{rel} - the reluctance torque component. The electromagnetic torque:

$$T_{el} = T_{ind} + T_{exc} + T_{rel} \quad (6)$$

From Equations 5 and 6, one can be observed that the electromagnetic torque of the LSPMSM is much more complex than that of the IM. Thus, the excitation torque and reluctance torque components are equivalent to those of the synchronous reluctance motor. The LSPMSM differs in that it includes an additional induction torque component, which plays a crucial role in the starting capability of the motor.

2.2. The Effect of PAU The structure of the LSPMSM can be considered as a combination of an IM and a PMSM with permanent magnets, as illustrated in Figure 3 (29).

In Equation 5 and Figure 3, it is indicated that the asynchronous torque T_{ind} of the LSPMSM is generated by the squirrel-cage part in the rotor found in the motor. When the LSPMSM operates in synchronous mode, the asynchronous torque component T_{ind} will be eliminated, leaving only the excitation torque component T_{exc} and the reluctance torque component T_{rel} . The asynchronous torque component T_{ind} generated during the starting process or during changes in rotational speed is collectively referred to as the transient process of the LSPMSM.

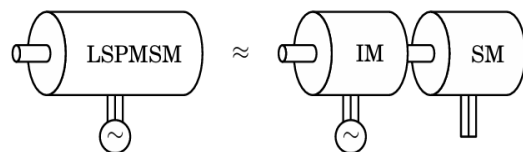


Figure 3. Structure of the LSPMSM

During the transient process, the LSPMSM is assumed to operate similarly to an IM with a slip coefficient “s”. The effect of PAU on the LSPMSM is most evident in its effect on the asynchronous torque T_{ind} during the transient process. When the power supply with VU, during the transient process, the asynchronous component can be analyzed into two components: the positive sequence and the negative sequence are shown in Figure 4 (30, 31).

When the LSPMSM operates in transient mode, it can be considered equivalent to an IM with a slip coefficient determined by the following expersion (32):

$$s = \frac{\omega_s - \omega_r}{\omega_s} \quad (7)$$

where: ω_s - the angular speed of the stator magnetic field, ω_r - the rotating speed of the rotor. When the three-phase power supply is unbalance, the slip coefficient, which includes the two components mentioned, is defined:

$$s^1 = \frac{\omega_s - \omega_r}{\omega_s} = 1 - \frac{\omega_r}{\omega_s}; s^2 = \frac{-\omega_s - \omega_r}{-\omega_s} = 1 + \frac{\omega_r}{\omega_s} \quad (8)$$

where: s^1 - positive sequence slip coefficient; s^2 - negative sequence slip coefficient (“1” corresponds to the positive sequence, “2” corresponds to the negative sequence). Assume:

$$K_u = \left(\frac{\omega_r}{\omega_s}\right) \quad (9)$$

Therefore:

$$s^1 = 1 - K_u; s^2 = 1 + K_u \quad (10)$$

The VU factor, K_V , is used to measure unbalance level. K_V is defined as the ratio of the negative sequence voltage component (V_n) to the positive sequence voltage

component (V_p). This definition aligns with the IEC 61000-4-30 standard (33).

$$K_V(\%) = \frac{V_n}{V_p} 100 \quad (11)$$

2. 2. 1. Effect on Torque

When the three-phase voltage is balance, the electromagnetic power of IM is defined as follows (32, 34):

$$P_{el} = 3 \frac{R'_r V_s^2}{s} (I'_r)^2 = \frac{3R'_r V_s^2}{s \left[\left(\frac{R'_r}{s} \right)^2 + (X'_r)^2 \right]} \quad (12)$$

Where: R'_r, X'_r - rotor resistance and rotor reactance converted to the stator side, V_s – voltage of stator, I'_r - rotor current converted to stator side.

Electromagnetic power with unconverted rotor parameter values:

$$P_{el} = \frac{3R_r V_s^2}{s \left[\left(\frac{R_r}{s} \right)^2 + (X_r)^2 \right]} \quad (13)$$

Where: R_r, X_r - resistor and reactance of rotor circuit. When there is PAU, the total electromagnetic power is defined as follows:

$$P_{el} = P_{el}^1 + P_{el}^2 \quad (14)$$

$$P_{el}^1 = \frac{3R_r (V_s^1)^2}{s^1 \left[\left(\frac{R_r}{s^1} \right)^2 + (X_r)^2 \right]} \quad P_{el}^2 = \frac{3R_r (V_s^2)^2}{s^2 \left[\left(\frac{R_r}{s^2} \right)^2 + (X_r)^2 \right]} \quad (15)$$

Where: V_s^1 and V_s^2 - positive sequence voltage component and negative sequence voltage component of stator.

Electromagnetic torque:

$$T = T^1 + T^2 = \frac{3R_r (V_s^1)^2}{s^1 \left[\left(\frac{R_r}{s^1} \right)^2 + (X_r)^2 \right] \omega_s} - \frac{3R_r (V_s^2)^2}{s^2 \left[\left(\frac{R_r}{s^2} \right)^2 + (X_r)^2 \right] \omega_s} \quad (16)$$

By applying the transformation, the torque can be calculated as follows:

$$T = \frac{3R_r (V_s^1)^2 (1 - K_u)}{[(R_r)^2 + (1 - K_u)^2 (X_r)^2] \omega_s} - \frac{3R_r (V_s^2)^2 (1 + K_u)}{[(R_r)^2 + (1 + K_u)^2 (X_r)^2] \omega_s} \quad (17)$$

When there is PAU, the starting torque is defined as follows:

$$T_{s_unbalance} = \frac{3R_r (V_s^1)^2}{[(R_r)^2 + (X_r)^2] \omega_s} - \frac{3R_r (V_s^2)^2}{[(R_r)^2 + (X_r)^2] \omega_s} \quad (20)$$

Compare with the starting torque when the three-phase balance voltage is defined by the following expression:

$$T_{s_balance} = \frac{3R_r V_s^2}{[(R_r)^2 + (X_r)^2] \omega_s} \quad (21)$$

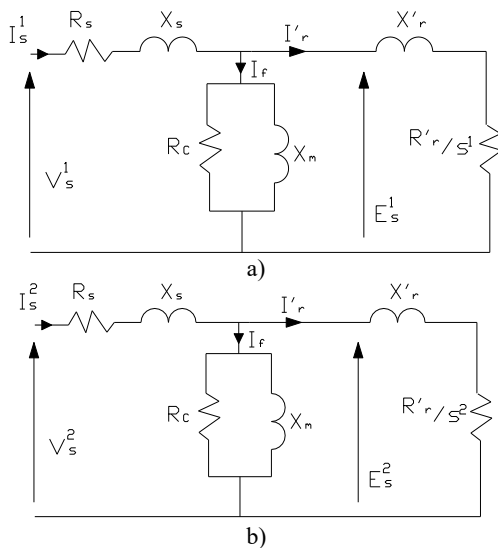


Figure 4. Equivalent circuit diagram of motor. (a) the positive sequence (b) the negative sequence of the motor

It can be observed that when there is PAU the asynchronous torque generated by the LSPMSM decreases by an amount equal to the negative sequence torque component. This results in the LSPMSM being more difficult to start and experiencing significant oscillations during the transient process.

2. 2. 2. Effect on Current and Losses The rotor current when the three-phase VU is defined as follows (32, 34):

$$I_r^2 = \frac{V_s^2}{\left(\frac{R_r}{s}\right)^2 + (X_r)^2} \quad (22)$$

When PAU occurs, the current on the rotor consists of two components: the positive sequence and the negative sequence, which are defined as follows:

$$(I_r^{1,2})^2 = \frac{(V_s^{1,2})^2}{\left(\frac{R_r}{s^{1,2}}\right)^2 + (X_r)^2} \quad (23)$$

The losses on the rotor are defined by the following formula:

$$\Delta P_{Cu2} = 3R_r I_r^2 = sP_{dt} = \frac{3R_r V_s^2}{\left[\left(\frac{R_r}{s}\right)^2 + (X_r)^2\right]} \quad (24)$$

When the power supply with PAU, the losses during oscillation include two components:

$$\Delta P_{Cu2}^{1,2} = \frac{3R_r (V_s^{1,2})^2}{\left[\left(\frac{R_r}{s^{1,2}}\right)^2 + (X_r)^2\right]} \quad (25)$$

The total load-loss on the rotor is determined:

$$\Delta P = \Delta P_{Cu2}^1 + \Delta P_{Cu2}^2 = \frac{3R_r (V_s^1)^2}{\left[\left(\frac{R_r}{s^1}\right)^2 + (X_r)^2\right]} + \frac{3R_r (V_s^2)^2}{\left[\left(\frac{R_r}{s^2}\right)^2 + (X_r)^2\right]} \quad (26)$$

From expression (26), it is indicated that when PAU occurs, the losses in the LSPMSM during the transients also increase by an amount equal to the negative sequence component that is generated.

3. THE EFFECT OF PAU ON THE LSPMSM

The subject of evaluation in this paper is the LSPMSM motor with the specifications: 15 kW, speed 3000 RPM, voltage (Δ/Y) 380/660 V. Detailed parameters are presented in Table 1 (27).

Ansys/Maxwell software was used to simulate LSPMSM. This software applies the Finite Element Method (FEM) for calculations. The motor model with Ansys/Maxwell is illustrated in Figure 5.

The PAU scenario for evaluating the performance of the LSPMSM is presented in Table 2.

3. 1. Research Results

3. 1. 1. Speed Characteristics The simulation results evaluating the starting quality of the LSPMSM

TABLE 1. LSPMSM parameters

Parameters	Symbol	Value	Unit
Stator Outer Diameter	D_{in}	245	mm
Stator inner diameter	D_{out}	152	mm
Rotor outer diameter	D'	151	mm
Rotor shaft diameter	D_r	52	mm
Stator steel material	<i>Steel 1008</i>		
Number of stator slots	Z_1	36	slots
Number of rotor slots	Z_2	28	slots
Air gap length	g	0,5	mm
Power supply voltage	U_n	380/660	V
Power supply frequency	f	50	Hz

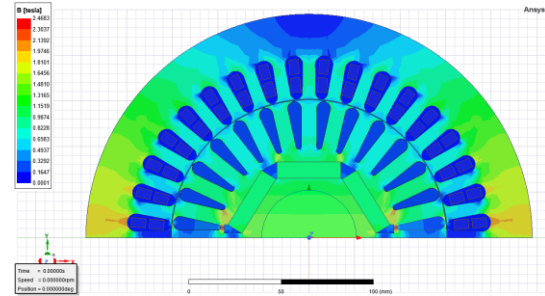


Figure 5. Simulation of the electromagnetic field distribution in the LSPMSM

TABLE 2. LSPMSM parameters

Scenarios	Alpha (α)	U_a, U_b, U_c
1	0°	
2	3°	$U_a = U_m \cdot \sin(\omega t)$
3	6°	$U_b = U_m \cdot \sin(\omega t - 120^\circ - \alpha)$
4	9°	$U_c = U_m \cdot \sin(\omega t - 240^\circ - \alpha)$
5	12°	

under power supply with PAU are presented in Figures 6 and 7.

The results shown in Figures 6 and 7 indicate that when the motor is supplied by a power with phase angle balance, it starts easily and operates in synchronous mode after the starting process. When the motor is supplied with the PAU, it becomes more difficult to start, and the motor does not operate in synchronous mode, exhibiting variations as the phase angle deviation increases. The quality of the LSPMSM's starting characteristic can be assessed through the basic parameters presented in Table 3.

From the results in Table 3, it can be observed that when the power supply to the motor is balance, the motor can starts and operates stably at synchronous speed after

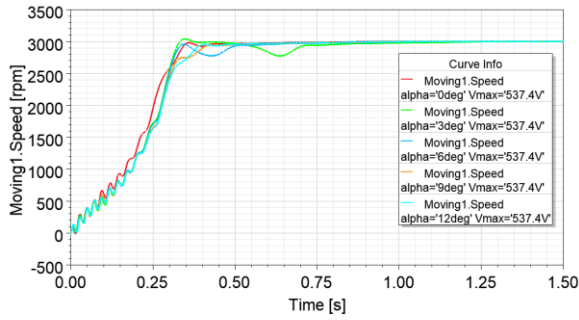


Figure 6. Speed characteristics of LSPMSM

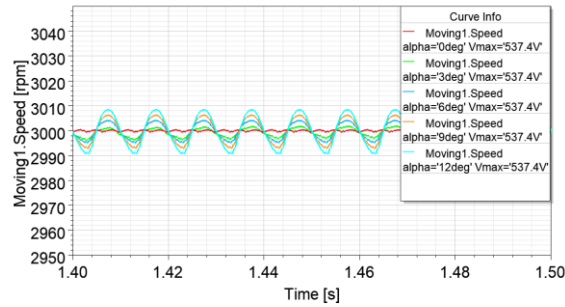


Figure 7. Speed characteristics of LSPMSM in steady state

TABLE 3. Parameters for evaluating the speed characteristics

Scenarios	Alpha (α)	Transient time t_{ts} (s)	Speed deviation $\Delta\omega$ (rpm)
1	0°	0.85	1
2	3°	1.26	2
3	6°	1.11	4
4	9°	1.12	6
5	12°	1.12	9

$t_{ts} = 0.85s$. When PAU occurs, the motor has more difficulty starting, with the maximum transient time $t_{ts} = 1.26s$ when the phase shift angle is $\alpha = 3^\circ$. Additionally, in steady-state mode, the motor runs with speed oscillations around synchronous speed; the larger the phase shift angle, the greater the speed fluctuation. The deviation is $\Delta\omega = 9$ rpm when the phase shift angle is $\alpha = 12^\circ$, compared to $\Delta\omega = 1$ rpm when there is no phase shift.

3. 1. 2. Torque Characteristics The simulation results evaluating the torque quality of the LSPMSM under power supply with PAU are presented in Figures 8 and 9.

The results shown in Figures 8 and 9 indicate that the motor torque exhibits oscillations even when the power supply is balance, although the level of oscillation is relatively low. However, when the power supply is

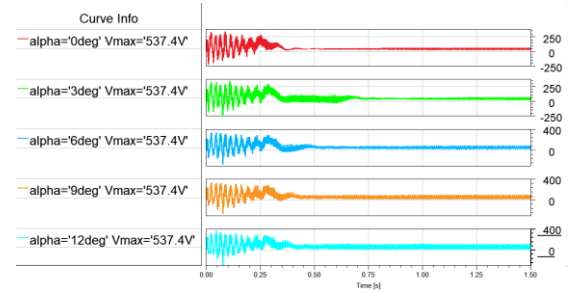


Figure 8. Torque characteristics of LSPMSM

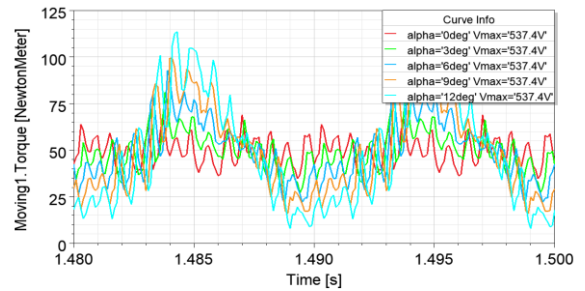


Figure 9. Torque characteristics of LSPMSM in steady state

unbalance in terms of phase angle, the motor torque experiences significant oscillations. This leads to vibrations and high noise levels during the operation of the motor. This is consistent with the theoretical analysis presented above.

To assess the level of torque ripple, some studies use the torque ripple coefficient k (35). The coefficient is defined through the values of maximum torque, minimum torque, and average torque. In summary, the formula (27) is used for calculating the torque ripple factor in the study as follows:

$$k = \frac{T_{\max} - T_{\min}}{T_{\text{avg}}} \quad (27)$$

Where, T_{\max} , T_{\min} represent the maximum and minimum value of instantaneous torque in an electric cycle, respectively, T_{avg} is the average value of the torque.

A summary of some parameters for evaluating the quality of working torque can be presented in Table 4.

TABLE 4. Parameters for evaluating the working torque

Scenarios	Alpha (α)	Transient time t_{ts} (s)	Torque ripple coefficient k
1	0°	0.85	0.89
2	3°	1.26	0.97
3	6°	1.11	1.34
4	9°	1.12	1.73
5	12°	1.12	2.21

The research results in Table 4 indicate that the transient time of torque increases when phase angle asymmetry occurs. As the degree of phase angle asymmetry increases, the coefficient k rises. The maximum value of the coefficient k is $k_{max} = 2.21$, corresponding to a phase shift angle of $\alpha = 12^\circ$, compared to $k = 0.89$ when there is no phase shift, indicating an increase of 2.48 times. This explains the phenomenon that the motor will operate with more vibrations and acoustic noise when phase angle asymmetry occurs.

3. 1. 3. Current Characteristics The simulation results of the current characteristics of the LSPMSM under power supply with PAU are presented in Figures 10 and 11.

The results in Figures 10 and 11 show that even when power supply with symmetrical three-phase voltage, the current of the LSPMSM still exhibits a high level of harmonics. However, when the power supply experiences PAU, the current waveform of the motor shows an even higher level of harmonics and take on a notched form. This demonstrates that the motor operates less efficiently, runs hotter, and may lead to motor failure. The harmonic order component analysis of the motor under VU of power supply is presented in Figure 12.

The total harmonic distortion index ($THDi$) is used to assess the level of harmonics in the current waveform, which is determined according to the following formula (31, 34):

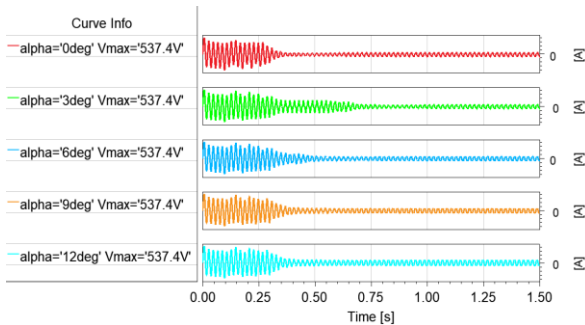


Figure 10. Current characteristics of phase A

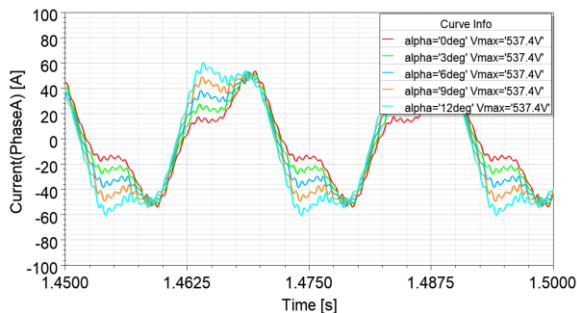


Figure 11. Current phase A in steady state

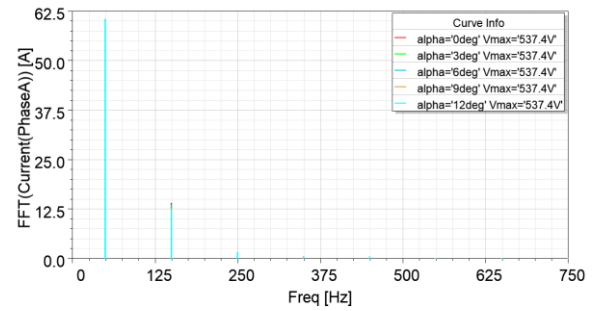


Figure 12. Analysis of the harmonic order of the current waveforms of the LSPMSM

$$THDi = \frac{\sqrt{\sum_{n=2}^{\infty} I_n^2}}{I_1} \tag{28}$$

The results of the $THDi$ assessment on a phase under conditions of PAU in the power supply are presented in Table 5.

The results in Table 5 show that as the phase shift angle increases, the $THDi$ of the motor's current wave forms also increases. The maximum harmonic index $THD_{imax} = 40.3$ corresponds to a phase shift angle of $\alpha = 9^\circ$. Beyond this point, further increases in the phase shift angle do not lead to an increase in $THDi$, which tends to remain approximately at the value of THD_{imax} .

Figure 13 below shows the waveforms of the currents in phases A, B, and C for the cases of $\alpha = 0^\circ$ và 12° .

From Figure 13(a), it can be seen that in the three-phase VB, the current waveforms of phases A, B, and C are similar and shifted by an angle of 120° . However, in Figure 13(b), when there is a PAU, the waveforms of the phases differ, and the phase shifts are also different (phase A with phase B is 216° , and phase B with phase C is 120°).

3. 1. 4. Efficiency and Power Factor The efficiency characteristics and power factor of the LSPMSM are investigated under conditions of PAU, with results presented in Figures 14 and 15.

The results of the efficiency and power factor in the steady state mode are provided in Table 6.

From the results in Table 6, one can be observed that the effect of PAU leads to increased losses, resulting in a

TABLE 5. Parameters for evaluating the working torque

Scenarios	Alpha (α)	THDi - Phase A
1	0°	35.8
2	3°	38.1
3	6°	39.5
4	9°	40.3
5	12°	40.2

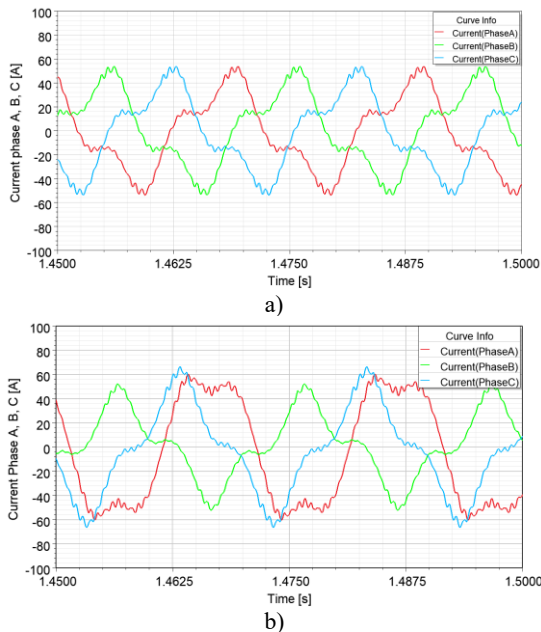


Figure 13. Current phase A, B, C in steady state. (a) $\alpha = 0^0$, (b) $\alpha = 12^0$

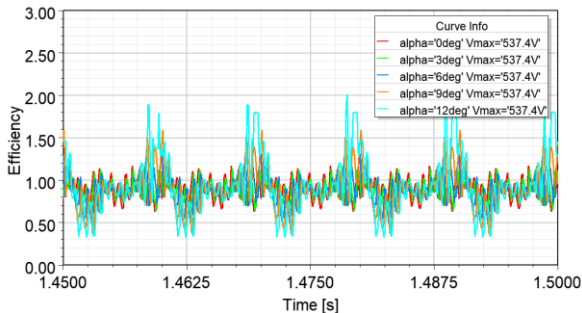


Figure 14. Efficiency characteristics of LSPMSM

decrease in the efficiency and power factor of the motor. When the phase shift angle is large, the efficiency of the

LSPMSM motor is even lower than that of the IM, which aligns with the theoretical basis analyzed previously.

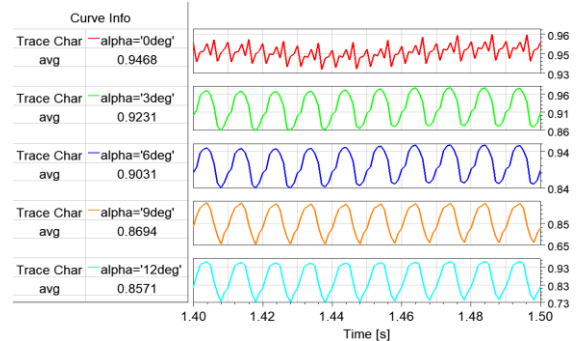


Figure 15. Power factor characteristics of LSPMSM

TABLE 6. Efficiency and power factor of LSPMSM

Scenarios	Alpha (α)	Efficiency η	Power factor $\text{Cos}\phi$
1	0^0	0.94	0.9468
2	3^0	0.93	0.9231
3	6^0	0.91	0.9031
4	9^0	0.89	0.8694
5	12^0	0.89	0.8571

4. EXPERIMENTAL STUDY IN THE LABORATORY

The experimental evaluation of the LSPMSM under conditions of power supply with PAU was conducted in the laboratory of the Department of Electrification at Hanoi University of Mining and Geology. Due to equipment limitations, the test results can only assess the current characteristics, efficiency, and power factor of the motor. The experimental setup is illustrated in Figure 16.

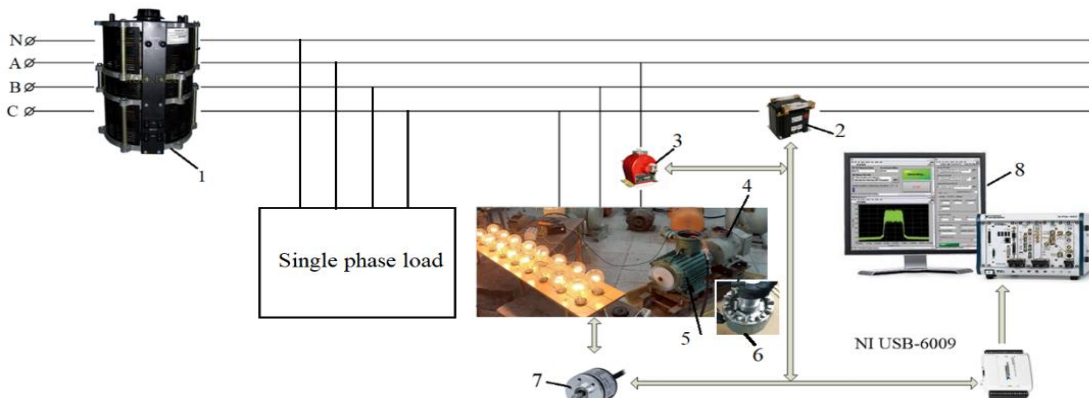


Figure 16. Experimental model of LSPMSM 1. Auto transformer, 2. Voltage transformer, 3. Current transformer, 4. Testing load, 5. Experimental LSPMSM, 6. Rotor of LSPMSM, 7. Encoder, 8. Displaying device

The testing process was conducted by adjusting a single-phase load to create PAU in the power supply to the LSPMSM. The single-phase load was adjusted so that the power supplied to the LSPMSM corresponds to a phase shift angle of 3^0 degrees. The steady-state current waveform characteristics obtained during the test for the case of 3^0 degree PAU are shown in Figure 16.

Figure 17 shows that the current characteristics exhibit a high level of harmonics and have a spike shape. This corresponds to the results obtained during the simulation using Ansys/Maxwell, as shown in Figure 11. The measured results for efficiency and power factor during the experiment are presented in Table 7.

The values obtained in the case of 3^0 -degree PAU in Table 6 are consistent with the values obtained in Table 5, with an error margin of 1.5% for efficiency and 1.2% for power factor. The analysis results in Figure 17 and Table also indicate that the experimental parameters are in line with the simulation results previously demonstrated regarding the impact of PAU on the operating conditions of the LSPMSM.



Figure 17. Current waveform characteristics under 3^0 -degree PAU

TABLE 7. Efficiency and power factor of LSPMSM

Scenarios	Alpha (α)	Efficiency η	Power factor $\text{Cos}\phi$
1	0^0	0.931	0.932
2	3^0	0.916	0.91

5. CONCLUSIONS

The LSPMSM has advantages in efficiency and high power factor, as well as the ability to self-start when powered, making it a subject of interest for research as a potential replacement for the widely used IM. LSPMSM motors are typically designed to operate with three-phase VB; however in operation, this motor is significantly affected by the quality of the power supply, where PAU unbalance is a relatively common phenomenon in the distribution network. Therefore, this paper focuses on

studying the phenomenon of PAU in a three-phase supply and its effect on the transient and steady-state processes of the LSPMSM. In addition to synthesizing theoretical analyses, the paper also conducts simulations using FEM application software and experiments on a 15 kW, 3,000 rpm LSPMSM model.

The analysis results show that when PAU occurs, the speed of the LSPMSM fluctuates significantly. At this point, the motor does not operate at synchronous speed and primarily operates in a transient mode. The LSPMSM becomes more difficult to start and may not be able to start at all, with the maximum transient time $t_{ts} = 1.26$ s in the case of a phase shift angle of $\alpha = 3^0$ degrees. The simulation results also indicate that as the phase shift angle increases, the speed deviation becomes larger, with a deviation of $\Delta\omega_0 = 9$ rpm corresponding to a phase shift angle of $\alpha = 12^0$, compared to $\Delta\omega = 1$ rpm when there is no phase shift. Additionally, an increase in PAU also leads to a higher oscillation torque coefficient k , which explains that the motor will operate with more vibration and acoustics noise when PAU occurs. Furthermore, the effect of PAU increases losses, reducing the efficiency and power factor of the motor. Thus, to enhance the operational efficiency of the LSPMSM, it is essential to implement measures to monitor the quality of the power supply provided to the LSPMSM to ensure efficiency and power factor during motor operation.

6. REFERENCES

1. Ang T-Z, Salem M, Kamarol M, Das HS, Nazari MA, Prabakaran N. A comprehensive study of renewable energy sources: Classifications, challenges and suggestions. *Energy strategy reviews*. 2022;43:100939. 10.1016/j.esr.2022.100939
2. Bobojanov M, Torayev S, editors. Saving electrical energy by using induction motors with pole changing windings in the water supply system. *E3S Web of Conferences*; 2023: EDP Sciences. 10.1051/e3sconf/202338401045
3. Saidur R. A review on electrical motors energy use and energy savings. *Renewable and sustainable energy reviews*. 2010;14(3):877-98. 10.1016/j.rser.2009.10.018
4. Isfahani AH, Vaez-Zadeh S. Line start permanent magnet synchronous motors: Challenges and opportunities. *Energy*. 2009;34(11):1755-63. 10.1016/j.energy.2009.04.022
5. Villani M, Santececca M, Parasiliti F, editors. High-efficiency line-start synchronous reluctance motor for fan and pump applications. 2018 XIII International Conference on Electrical Machines (ICEM); 2018: IEEE. 10.1109/ICELMACH.2018.8507230
6. Chaudhari M CA. Improved Performance Analysis of Single-phase Line Start Synchronous Reluctance Motor Derived from Induction Motor. *International Journal of Engineering Transactions B: Applications*. 2022;35(8):1641-50. 10.5829/ije.2022.35.08b.20
7. Ferreira F, De Almeida A, Cistelecán M, editors. Voltage unbalance impact on the performance of line-start permanent-magnet synchronous motors. *Proceedings of the 6th International Conference EEMODS, Nantes, France*; 2009.

8. Knezevic BZ. Analysis of Voltage Asymmetry in Mechatronic Systems: Modeling and Experimental Validation. Proceedings of VIAC in October 2023. 2023:74.
9. Tshoombe BK, Tabora JM, da Silva Fonseca W, Tostes MEL, de Matos EO, editors. Voltage harmonic impacts on line start permanent magnet motor. 2021 14th IEEE International Conference on Industry Applications (INDUSCON); 2021: IEEE. 10.1109/INDUSCON51756.2021.9529539
10. Gnaciński P, Muc A, Pepliński M. Influence of voltage subharmonics on line start permanent magnet synchronous motor. IEEE Access. 2021;9:164275-81. 10.1109/ACCESS.2021.3133279
11. Chingale G, Ugale R, editors. Harmonic filter design for line start permanent magnet synchronous motor. 2014 International Conference on Advances in Electrical Engineering (ICAEE); 2014: IEEE. 10.1109/ICAEE.2014.6838503
12. Ugale R, BalaKrishna Y, Chaudhari B, editors. Effects of short power interruptions and voltage sags on the performance of line start permanent magnet synchronous motor. 2008 4th IET Conference on Power Electronics, Machines and Drives; 2008: IET. 10.1049/cp:20080508
13. Qiu H, Hu K, Yi R, Yanqi W. Effect of high frequency harmonic voltage on the performance of line start permanent magnet synchronous motor. COMPEL-The international journal for computation and mathematics in electrical and electronic engineering. 2019;38(2):777-92. 10.1108/COMPEL-06-2018-0267
14. Gnacinski P, Peplinski M, Muc A, Hallmann D. Line-Start Permanent Magnet Synchronous Motor Supplied with Voltage Containing Negative-Sequence Subharmonics. Energies. 2024;17(1). 10.3390/en17010091
15. Idziak P, Nowak M, Pietrowski W. Spectral analysis of phase currents of LSPMSM at asymmetric voltage supply. Pomiary Automatyka Kontrola. 2013;59.
16. Sethupathi P, Senthilnathan N, Ravisanakar B, Lenin N. Voltage harmonics impact on line start permanent magnet synchronous motor: a new computational method. Arabian Journal for Science and Engineering. 2022;47(11):14377-88. 10.1007/s13369-022-06764-y
17. Sethupathi P, Senthilnathan N. Comparative analysis of line-start permanent magnet synchronous motor and squirrel cage induction motor under customary power quality indices. Electrical Engineering. 2020;102(3):1339-49. 10.1007/s00202-020-00955-2
18. Paramonov A, Oshurbekov S, Kazakbaev V, Prakht V, Dmitrievskii V. Investigation of the effect of the voltage drop and cable length on the success of starting the line-start permanent magnet motor in the drive of a centrifugal pump unit. Mathematics. 2023;11(3):646. 10.3390/math11030646
19. Maraaba L, Al-Hamouz Z, Milhem A, Abido M. Modelling of interior-mount LSPMSM under asymmetrical stator winding. IET Electric Power Applications. 2018;12(5):693-700. 10.1049/iet-epa.2017.0525
20. Jedryczka C, Wojciechowski RM, Demenko A. Finite element analysis of the asynchronous torque in LSPMSM with non-symmetrical squirrel cage winding. International Journal of Applied Electromagnetics and Mechanics. 2014;46(2):367-73. 10.3233/JAE-141947
21. Maraaba LS, Al-Hamouz ZM, Abido MA, editors. Modeling and simulation of line start permanent magnet synchronous motors with asymmetrical stator windings. IECON 2016-42nd Annual Conference of the IEEE Industrial Electronics Society; 2016: IEEE. 10.1109/IECON.2016.7793412
22. Gherabi Z, Toumi D, Benouzza N, Bendiabdellah A. A proposed approach for separation between short circuit fault, magnetic saturation phenomenon and supply unbalance in permanent magnet synchronous motor. International Journal of Engineering Transactions A: Basics. 2020;33(10):1968-77. 10.5829/ije.2020.33.10a.15
23. Ugale RT, Chaudhari BN, Pramanik A. Overview of research evolution in the field of line start permanent magnet synchronous motors. IET Electric Power Applications. 2014;8(4):141-54. 10.1049/iet-epa.2013.0241
24. Huang J, Wang C. Influence of rotor structures on line-start permanent magnet machines electromagnetic characteristics for pumping units application. International Journal of Applied Electromagnetics and Mechanics. 2020;63(2):375-90. 10.3233/JAE-190093
25. Qiu H, Hu K, Yang C. Influence of Wye-and Delta-Connected Winding on the Performance of Line Start Permanent-Magnet Synchronous Motor. International Journal of Emerging Electric Power Systems. 2018;19(6):20180097. 10.1515/ijeeps-2018-0097
26. Fonseca D, Antunes HR, Cardoso AJM, editors. Line-Start Permanent Magnet Synchronous Motors Stator Fault Diagnostics Immune to Unbalanced Supply Voltages. 2024 International Conference on Electrical Machines (ICEM); 2024: IEEE. 10.1109/ICEM60801.2024.10700193
27. Do Nhu Y, Thuy TB, Cuong NX. Rotor Configuration for Improved Working Characteristics of Lspmsm in Mining Applications. Natsional'nyi Hirnychiy Universytet Naukovyi Visnyk. 2024(3):79-86. 10.33271/nvngu/2024-3/079
28. Mahmoudi A, Roshandel E, Kahourzade S, Vakiliipoor F, Drake S. Bond graph model of line-start permanent-magnet synchronous motors. Electrical Engineering. 2024;106(2):1667-81. 10.1007/s00202-022-01654-w
29. Modeer T. Modeling and testing of line start permanent magnet motors: KTH; 2007.
30. Chauhan A, Thakur P, Raveendhra D. Quantification of voltage unbalance conditions. Power Electronics and Renewable Energy Systems: Proceedings of ICPERES 2014: Springer; 2014. p. 47-55.
31. Deleanu S, Von Lipinski G, Iordache M, Stanculescu M, Niculae D, editors. Performance Evaluation of the Three-Phase Induction Motor Operating in Conditions of Unbalanced Voltage Supply. 2019 8th International Conference on Modern Power Systems (MPS); 2019: IEEE. 10.1109/MPS.2019.8759684
32. Bhattarai PD. Study on effects of supply voltage asymmetry and distortion on induction machine: Louisiana State University and Agricultural & Mechanical College; 2013.
33. Commission IE. IEC 61000-4-30, Electromagnetic compatibility (EMC)-Part 4-30: Testing and measurement techniques-Power quality measurement methods. International Electrotechnical Commission: Geneva, Switzerland. 2015.
34. Neves ABF, de Mendonça MVB, de Leles Ferreira Filho A, Rosa GZ, editors. Effects of voltage unbalance and harmonic distortion on the torque and efficiency of a Three-Phase Induction Motor. 2016 17th International Conference on Harmonics and Quality of Power (ICHQP); 2016: IEEE. 10.1109/ICHQP.2016.7783350
35. Song S, Fang G, Hei R, Jiang J, Ma R, Liu W. Torque ripple and efficiency online optimization of switched reluctance machine based on torque per ampere characteristics. IEEE Transactions on Power Electronics. 2020;35(9):9608-16. 10.1109/TPEL.2020.2974662

COPYRIGHTS

©2026 The author(s). This is an open access article distributed under the terms of the Creative Commons Attribution (CC BY 4.0), which permits unrestricted use, distribution, and reproduction in any medium, as long as the original authors and source are cited. No permission is required from the authors or the publishers.



Persian Abstract

چکیده

امروزه، موتورهای سنکرون آهنربای دائم راه‌اندازی خط (LSPMSM) به عنوان جایگزینی جزئی برای موتورهای القایی برای اهداف صرفه‌جویی در مصرف انرژی مورد بررسی قرار می‌گیرند. LSPMSM معمولاً برای کار با تعادل ولتاژ سه فاز (VB) طراحی شده است. در حال حاضر، با بارهای تک فاز، پدیده عدم تعادل زاویه فاز (PAU) به طور مکرر در شبکه توزیع رخ می‌دهد که پارامترهای کاری موتور را خراب می‌کند و ممکن است منجر به آسیب در حین کار شود. بنابراین، محتوای این مقاله بر بررسی تأثیر PAU در شبکه توزیع بر ویژگی‌های کاری LSPMSM 15 kW0-3,0 تمرکز دارد. نتایج تجزیه و تحلیل نشان می‌دهد که وقتی PAU رخ می‌دهد، LSPMSM برای شروع مشکل بیشتری دارد و ممکن است شروع نشود. سرعت LSPMSM به شدت نوسان می‌کند، با سرعت همزمان کار نمی‌کند و عمدتاً در فرآیند گذرا کار می‌کند. در طول فرآیند گذرا منجر به ضریب گشتاور نوسانی بالاتر k می‌شود، که توضیح می‌دهد که موتور با نویز ارتعاش و آکوستیک بیشتری کار می‌کند. علاوه بر این، اثر PAU باعث افزایش تلفات و کاهش راندمان و ضریب قدرت موتور می‌شود. این مقاله این اثر را از طریق مدل‌های شبیه‌سازی و آزمایش تجربی در آزمایشگاه برای LSPMSM ارزیابی می‌کند. نتایج نشان می‌دهد که مبنای نظری سنتز شده در مقاله برای مطالعه مناسب است.
